European Journal of Sustainable Development Research
2026, 10(4), em0429
e-ISSN: 2542-4742
https://www.ejosdr.com/

MODESTUM

Research Article

OPEN ACCESS

Climate change impacts on the thermal performance of passive envelopes under varying air infiltration rates: Multi-scale analysis in Marrakech

Houcine Kasmi [1*], Ouadia Mouhat [1]

[1] Civil Engineering and Environment Laboratory, Mohammadia School of Engineers, Mohammed V University in Rabat, MOROCCO
***Corresponding Author:** houcine_kasmi@um5.ac.ma

Citation: Kasmi, H., & Mouhat, O. (2026). Climate change impacts on the thermal performance of passive envelopes under varying air infiltration rates: Multi-scale analysis in Marrakech. *European Journal of Sustainable Development Research, 10*(4), em0429. https://doi.org/10.29333/ejosdr/19112

ARTICLE INFO

Received: 13 May 2026

Accepted: 06 Jul. 2026

ABSTRACT

The long-term thermal performance of residential buildings, as well as the thermal comfort of their occupants, is strongly dependent on external climatic conditions. In this context, this study investigates the evolution of thermal comfort in a representative residential dwelling located in Marrakech under current (2020) and future climate conditions (2050 and 2080) based on the Representative Concentration Pathway (RCP) 8.5 scenario. Dynamic simulations were conducted using EnergyPlus under free-running conditions to isolate envelope-related thermal behaviour. Five envelope configurations were evaluated: a reference case without thermal efficiency measures, a configuration incorporating expanded polystyrene (EPS) insulation, a configuration using double low-emissivity tinted glazing (6/13/6), a phase change material (PCM) configuration, and a combined strategy integrating multiple passive measures. Each configuration was assessed under three air infiltration rates (0, 1.5, and 2.2 ACH), with thermal comfort analysed at both building and room scales, resulting in a simulation matrix of 135 configurations. Results show a clear shift from a mixed discomfort regime, where both underheating and overheating occur, toward conditions increasingly dominated by overheating. In the baseline case (reference envelope, 1.5 ACH), overheating-related discomfort rises from 36% of annual hours in 2020 to 51% in 2080, largely driven by extreme overheating events. Envelope strategies show contrasting performance: insulation improves winter comfort but promotes heat retention under warmer climates; glazing reduces peak overheating in solar-exposed spaces; and phase change materials provide limited benefit due to insufficient night cooling. The combined strategy performs best, reducing extreme overheating by up to 986 h/year, although its effectiveness declines under late-century conditions. Room-level analysis further reveals substantial spatial variability, with highly exposed rooms experiencing overheating levels more than 30% above whole-building estimates. These findings highlight the need for integrated passive design strategies that account for airtightness, spatial variability, and future climate conditions.

Keywords: climate change, overheating, thermal comfort, passive envelope strategies, infiltration, building resilience

INTRODUCTION

The thermal performance of buildings is largely influenced by outdoor climatic conditions, and climate change is considered a major factor affecting their thermal behaviour, thereby causing shifts in indoor thermal conditions and, consequently, changes in occupants' thermal comfort (Machard et al., 2023; Salata et al., 2023). Hot, arid, and semi-arid regions, which are characterized by high outdoor temperatures, are particularly affected by this trend, notably the North African region, which, according to the Intergovernmental Panel on Climate Change (IPCC), is identified as an area highly vulnerable to climate change, with projected increases in air temperature, more frequent and prolonged heat waves, and significantly higher nighttime temperatures under high-emission scenarios such as RCP 8.5 (Barkhordarian et al., 2011; IPCC, 2021) More specifically, regional studies indicate that Moroccan cities could experience a substantial increase in extreme heat events by the middle and end of the century, raising concerns regarding indoor thermal comfort and the resilience of residential buildings (Driouech et al., 2020).

As Marrakech is one of the cities characterized by a semi-arid climate, residential buildings in this city are becoming increasingly exposed to extreme climatic conditions due to the progressive rise in outdoor temperatures, which directly influences indoor thermal conditions, often leading to overheating and reducing the effectiveness of conventional design approaches. As a result, buildings designed based on historical climate data may no longer provide adequate performance under future conditions. To improve indoor thermal conditions, both passive and active systems are used to maintain acceptable indoor environments. However, the use of active systems, such as mechanical cooling, masks the intrinsic thermal behaviour of building envelopes, as these systems compensate for thermal imbalances through active control. For this reason, free-running simulation approaches are commonly adopted in building performance studies to evaluate the inherent response of envelope systems without mechanical intervention (Delgado-Gutierrez et al., 2025; Machard et al., 2003). Such approaches allow a direct assessment of the contribution of envelope design to the overall thermal behaviour of buildings.

The use of passive envelope systems, including thermal insulation, high-performance glazing, and phase change materials (PCM), is widely considered a key solution for improving building performance by acting on key parameters such as regulating heat transfer, reducing peak thermal loads, and enhancing the thermal stability of indoor environments (AMEE, 2015; Eddib & Lamrani, 2019; Kharbouch, 2022; Khechiba et al., 2023). In Morocco, these measures are encouraged through regulatory instruments such as the Moroccan Thermal Regulation for Construction (RTCM) (AMEE, 2015), which aims to improve envelope performance in residential buildings. However, their effectiveness is strongly influenced by climatic conditions and boundary parameters, and may vary significantly under future climate scenarios (Aruta et al., 2025; Diab et al., 2025; Flores-Larsen et al., 2019; Kasmi & Mouhat, 2026; Rodrigues & Fernandes, 2020; Villano et al., 2026).

In addition to envelope characteristics, air infiltration represents a parameter that is gaining increasing attention, as it plays a significant role in the thermal performance of buildings by influencing heat exchange between indoor and outdoor environments (Ng et al., 2015). Depending on external conditions, infiltration can either contribute to passive cooling or increase thermal loads, and therefore requires further investigation.

Furthermore, thermal performance simulation is largely conducted at the whole-building scale, which may not adequately capture significant spatial variations within the building. Differences in orientation, solar exposure, and occupancy patterns can lead to heterogeneous thermal behaviour across different zones, particularly in hot climates where solar gains are dominant (Arriazu-Ramos et al., 2023).

Given these challenges, it has become increasingly important to take these aforementioned assumptions into consideration in order to better understand the actual behaviour of each building parameter, whether considered independently or in interaction with other parameters, thereby forming a multi-parameter and multi-combination assessment framework.

Thermal insulation, particularly through the use of synthetic insulating materials such as expanded polystyrene (EPS), is widely applied to improve building performance by reducing heat transfer through the building envelope. The use of this type of insulation has demonstrated remarkable effectiveness in reducing heating demand. However, its behaviour in hot climates remains less consistent. In this context, several studies indicate that insulation may contribute to heat accumulation during summer periods when nighttime heat dissipation is insufficient, particularly under future climate scenarios (Fosas et al., 2018).

Glazing systems also contribute significantly to building performance by reducing solar heat gain while allowing sufficient natural daylight indoors. Their effectiveness, however, depends on several factors, particularly façade orientation, glazing surface area, and the thermal and optical properties of the glazing material. In practice, choosing the most suitable glazing type requires finding the right balance between solar protection and daylight access. For this reason, glazing design should be carefully adapted to local climatic conditions and building configuration to ensure optimal thermal performance (Pérez-Carramiñana et al., 2022).

Phase change materials (PCM) have been proposed to enhance the thermal storage capacity of building envelopes through latent heat processes. Several studies have shown that properly integrated PCM can reduce peak indoor temperatures and attenuate thermal fluctuations (Salihi et al., 2024; Suresh et al., 2022). However, their thermal behaviour is strongly influenced by climatic conditions, which determine both the phase transition process and the effectiveness of daily regeneration cycles (Kuznik et al., 2011; Salihi et al., 2022). In hot climates, elevated night-time temperatures may limit complete solidification, thereby reducing the overall thermal storage efficiency. These constraints highlight the need for careful selection of PCM properties in relation to local climatic conditions.

The thermal response of buildings is subject to uncertainty due to air infiltration, which is often underestimated in modelling approaches. Air infiltration is largely uncontrolled and can fluctuate over time due to construction imperfections, ageing and variable environmental conditions. In certain situations, air exchange can contribute to heat dissipation, particularly when temperature differences between the interior and exterior are favourable. However, in warmer conditions, it can instead exacerbate heat accumulation and reduce indoor thermal stability, as it can increase internal heat loss during colder winter periods (Ng et al., 2015). Despite this dynamic and uncertain behaviour, air infiltration is often treated as a simplified or fixed parameter, which limits the ability of simulation models to capture its actual influence, particularly when combined with other building envelope design strategies.

Furthermore, most studies assess building performance using aggregated indicators at the whole-building level. However, several works demonstrate that thermal behaviour can vary significantly within different zones of the same building, particularly due to orientation and solar exposure differences. As a result, building-level evaluations may underestimate localized thermal stress, emphasizing the need for room-level analysis to capture spatial variability (Arriazu-Ramos et al., 2023).

Recent studies have investigated the influence of climate change, passive envelope technologies, air infiltration, and building thermal performance. However, these aspects are often examined independently, with limited attention to their combined interactions and their influence on both heating- and cooling-related thermal behaviour (Kitsopoulou et al., 2024; Kutty et al., 2023; Mohammed et al., 2024). In particular, air infiltration is frequently represented using fixed assumptions, despite its strong influence on heat gains, heat losses, and indoor thermal conditions. Likewise, thermal performance assessments are commonly conducted either at the whole-building scale or under a single infiltration or ventilation scenario, which may obscure the combined effects of infiltration variability, passive envelope measures, climatic evolution, and room-specific exposure.

Consequently, the combined influence of future climate conditions, variable air infiltration rates, passive envelope adaptation mesures, and spatial-scale thermal response remains insufficiently understood, particularly in hot semi-arid residential contexts where climate change is expected to intensify thermal stress and modify the balance between heating and cooling requirements (Zhang et al., 2024).

The present study addresses this gap through the integrated assessment of four dimensions that are still rarely examined simultaneously within a unified dynamic simulation framework for residential buildings in hot semi-arid climates. These dimensions include: (i) the comparative evaluation of individual and combined passive envelope strategies; (ii) the consideration of air infiltration rate variability (0, 1.5 and 2.2 ACH), as a variable parameter rather than a fixed assumption; (iii) the multi-scale assessment of thermal performance at both building and room levels; and (iv) the analysis of these interactions under both current and future climate conditions (2020, 2050, and 2080). The proposed framework enables the evaluation of the effectiveness and robustness of passive design measures under different infiltration conditions and future climatic stress levels, while revealing thermal vulnerabilities that may remain hidden when only building-average indicators are considered (Arriazu-Ramos et al., 2023; Choi et al., 2023; Machard et al., 2023; Salihi et al., 2024).

Specifically, this study aims to :

- Analyse the evolution of building thermal performance under present and future climate scenarios (2020, 2050, and 2080) based on the RCP 8.5 pathway;
- Assess the individual and combined effects of passive envelope technologies, including thermal insulation (EPS), high-performance glazing, and phase change materials (PCM);
- Investigate the influence of air infiltration variability on building thermal behaviour under different climatic conditions;
- Compare thermal performance at both building and room scales in order to capture spatial heterogeneity;
- Evaluate the robustness of passive envelope strategies under increasing thermal stress conditions and varying air infiltration rates.

Marrakech is employed as a representative climatic case study through which the interaction between passive envelope strategies, infiltration variability, and climate change can be systematically investigated. Although the quantitative outcomes are influenced by the characteristics of the investigated building and climatic context, the adopted framework is intended to provide transferable insights into the physical mechanisms and design trade-offs governing thermal performance and thermal resilience in residential buildings located in comparable hot semi-arid regions (Delgado-Gutierrez et al., 2025; Kharbouch, 2022; Salata et al., 2023).

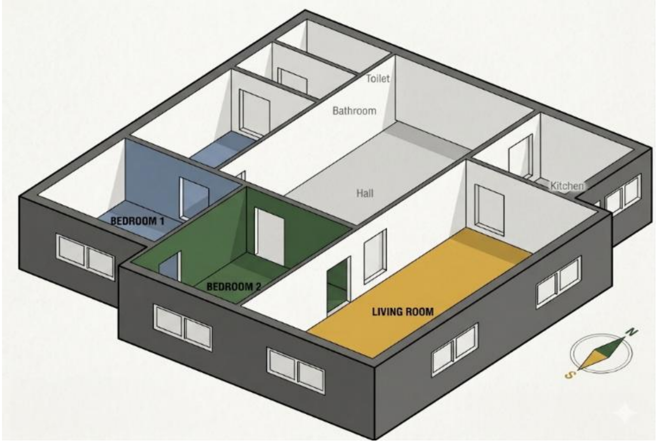

Figure 1. Geometry and architectural layout of the case study residential building (Source: Authors' own elaboration)

MATERIALS AND METHODS

Case Study Building and Architectural Characteristics

This study considers a representative residential building located in Marrakech, Morocco (31.63°N, 8.00°W), wich is a region characterized by a hot arid climate (BWh, Köppen classi-fication). The studied building consists of two main east-and south-facing façades comprising three storeys (ground floor and two upper floors), with a ceiling height of 3.5 m on all floors, each with a net floor area of approximately 100 m², giving a total gross floor area of approximately 300 m².

Figure 1 illustrates the typical layout of a floor, which comprises two bedrooms, a living room, a kitchen, a bathroom and a toilet.

In order to focus on the intrinsic thermal behaviour of the building envelope, this study does not take into account external influencing factors such as surrounding buildings, vegetation and shading devices

This modelling choice facilitates a clearer interpretation of envelope-related thermal response by reducing the influence of external contextual factors and enables more direct comparison of passive strategy performance under future climatic stress.

Although the present study is based on a specific representative residential building, the adopted simulation framework was designed to support broader understanding of passive envelope behaviour under future climatic stress. Recent simulation-based studies suggest that building performance assessments developed for individual cases may provide transferable methodological insights when key context-dependent parameter, such as climatic conditions, envelope characteristics, occupancy assumptions, and air exchange conditions, are adapted to comparable settings (Rodrigues et al., 2024; Romero-Recuero et al., 2025).

Spatial Scale of Thermal Comfort Analysis

Thermal comfort was analysed at three complementary spatial scales to capture both global and local thermal behaviour:

- Building level, representing the aggregated thermal response of the entire dwelling;
- Bedroom, a west-oriented room with a floor area of approximately 9.6 m^2 (3.0 m × 3.2 m). This room was selected due to its high exposure to afternoon solar gains, which are particularly critical in hot arid climates, and because of its importance for night-time thermal comfort;
- Living room, a dual-aspect space oriented east and south, with a floor area of approximately 32 m^2 (4.0 m × 8.0 m), representative of spaces subjected to prolonged solar exposure throughout the day.

This multi-scale and orientation-sensitive approach allows the identification of spatial heterogeneity in thermal comfort conditions, which may remain hidden when assessments rely solely on building-average indicators. Considering room-level thermal response also facilitates a more detailed interpretation of thermal performance associated with orientation, solar exposure, and local indoor conditions, as highlighted in recent studies emphasizing spatial variability in residential thermal performance (Xie et al., 2025).

Climate Data and Future Scenarios

Three climatic horizons were considered in the simulations:

- 2020, representing current reference climatic conditions;
- 2050, representing mid-century climate projections;
- 2080, representing late-century climate projections.

Future weather files were generated using Meteonorm software version 8, which pro-vides statistically consistent future climate projections derived from global climate models and widely adopted morphing techniques. Meteonorm has been extensively validated and is commonly used in building performance and climate adaptation studies (Belcher et al., 2005; Hatwaambo et al., 2009). Its application ensures methodological consistency with established procedures for generating future weather files suitable for dynamic thermal simulation.

Future climate scenarios were based on the RCP 8.5, corresponding to a high-emission trajectory (IPCC, 2014). This scenario is commonly adopted in studies addressing building resilience and overheating risk to assess worst-case climatic conditions. The use of multiple future horizons enables the evaluation of the evolution of thermal comfort performance under progressively increasing thermal stress, which is particularly relevant for long-term climate adaptation planning in hot arid and semi-arid regions.

Envelope Configurations and Passive Design Strategies

The influence of passive envelope strategies on thermal comfort was investigated by focusing on three key parameters:

- Thermal insulation of external walls and roof using expanded polystyrene (EPS);
- Window glazing performance, comparing simple glazing with high-performance double glazing;
- Integration of phase change materials (PCM) within external wall and roof assemblies.

In this study, each passive strategy was treated as a binary parameter, "0": absence of the strategy (reference condition), and "1": full application of the strategy.

This binary representation was intentionally adopted to improve clarity, enhance physical interpretability of results, and focus on the robustness of passive strategies under current and future climate conditions.

Based on this framework, five envelope configurations were analysed:

- 0–0–0: reference configuration with no insulation, conventional glazing, and no PCM;
- 1–0–0: insulation-only configuration, with EPS applied to external walls and roof;
- 0–1–0: glazing-only configuration, with high-performance double glazing ap-plied to all windows;
- 0–0–1: PCM-only configuration, with PCM integrated into external walls and roof;
- 1–1–1: combined configuration, integrating insulation, high-performance glazing, and PCM.

The adopted configuration framework enables the separate and combined influence of major passive envelope strategies to be examined under identical climatic and operational conditions. This facilitates a clearer interpretation of their relative contribution to thermal comfort performance and supports the identification of robust passive design combinations under increasing climatic stress, as emphasized in recent studies on climate-responsive envelope adaptation.

Infiltration and Natural Ventilation Modelling

Air infiltration was modelled as a constant air change rate (ACH) to represent uncontrolled air leakage through the building envelope. In residential buildings, infiltration is primarily driven by envelope airtightness, construction quality, and ageing effects rather than deliberate design control. Although infiltration is physically dependent on wind speed and temperature-driven pressure differences, the use of constant ACH values is widely adopted in building performance simulations to represent envelope leakage under simplified and comparable boundary conditions (Choi et al., 2023; Younes et al., 2011).

Three infiltration scenarios were defined:

- 0 ACH, representing an idealised airtight condition;
- 1.5 ACH, representing moderate infiltration typical of conventional residential construction;
- 2.2 ACH, representing poor airtightness conditions associated with ageing or low construction quality.

These values were selected to capture the variability commonly reported in field measurements of residential airtightness. The chosen range therefore enables evaluation of envelope performance under realistic construction variability while maintaining methodological comparability across climatic horizons. The inclusion of a zero-infiltration scenario provides a theoretical benchmark for assessing the intrinsic thermal behaviour of the envelope independent of uncontrolled air exchange.

The inclusion of multiple infiltration levels allows assessment of thermal comfort sensitivity to envelope leakage uncertainty, which remains one of the least controlled parameters in residential buildings.

Infiltration was therefore treated as an uncertain and largely uncontrollable parameter, rather than an optimisation variable. This approach enables evaluation of the robustness of passive envelope strategies under realistic construction variability.

Natural ventilation was modelled separately and fixed at 0.6 ACH across all thermal zones and scenarios. This value represents a baseline ventilation rate independent of occupant-driven window operation. Maintaining a constant background ventilation rate ensures methodological consistency and isolates the effects of envelope configuration, infiltration variability, and climatic evolution.

Adaptive, demand-controlled, or occupant-responsive ventilation strategies were intentionally excluded from the analysis. The objective of this study is to evaluate intrinsic envelope performance under standardized airflow conditions, rather than to optimise behavioural or operational strategies. This controlled modelling framework enhances comparability across scenarios and prevents behavioural variability from confounding envelope-related performance assessment.

Although pressure-based infiltration models provide dynamic airflow estimation, the constant ACH approach was adopted to ensure scenario comparability and to focus on envelope thermal performance rather than airflow modelling complexity.

Simulation Tool and Modelling Assumptions

Dynamic thermal simulations were performed using DesignBuilder software (version 7), employing the EnergyPlus simulation engine. EnergyPlus is a validated and widely adopted whole-building dynamic simulation tool capable of modelling transient heat transfer, solar gains, airflow, and phase change material behaviour under detailed boundary conditions (Bastos Porsani & Fernández Bandera, 2023).

All simulations were performed under free-running conditions, without active heating or cooling systems, to isolate the intrinsic thermal response of envelope configurations and passive air exchange mechanisms. Such an approach enables the assessment of passive thermal behaviour without the compensating influence of HVAC operation and has been adopted in recent studies investigating building thermal performance under future climate conditions (Amraoui et al., 2025).

Numerical and physical modelling settings

The following modelling settings were applied:

- Time step: 1 hour reporting interval with sub-hourly internal calculation steps as defined by EnergyPlus default convergence algorithms;
- Heat balance algorithm: Conduction Transfer Function (CTF) method for opaque constructions;
- Solar distribution: Full interior and exterior solar distribution;
- Convection model: Adaptive convection algorithm (EnergyPlus default);
- Long-wave radiation exchange: Surface-to-surface radiation model;
- Ground boundary condition: Slab-on-grade ground model with constant deep ground temperature derived from climatic data;
- Warm-up period: Automatic warm-up iterations until annual heat balance convergence.

For PCM-integrated assemblies, the enthalpy–temperature function method implemented in EnergyPlus (MaterialProperty:PhaseChange) was used to simulate latent heat storage behaviour. Temperature-dependent thermal properties were defined according to manufacturer data in **Table 1**.

Internal gains and occupancy

Identical internal gains and occupancy schedules were applied across all scenarios to ensure comparability. Internal loads included:

- Sensible heat gains from occupants;
- Lighting loads;
- Equipment loads representative of residential usage.

Occupancy and internal gain profiles were maintained constant across climatic hori-zons and envelope configurations to isolate the effects of passive strategies and climate evolution.

Boundary conditions and scenario consistency

Material properties were kept fixed for each envelope configuration. Climatic boundary conditions varied only according to the selected weather file (2020, 2050, 2080), while all other operational parameters remained unchanged.

This controlled modelling framework ensures reproducibility and enables direct comparison of envelope strategy performance across infiltration levels and climatic horizons.

Thermal Comfort Indicators and Discomfort Metrics

Thermal comfort was assessed using hourly operative temperature, which combines indoor air temperature and mean radiant temperature. Operative temperature is widely adopted in the assessment of free-running buildings, as it captures both convective and radiative heat exchange between occupants and surrounding surfaces and provides a physically meaningful indicator of thermal exposure.

The evaluation was conducted under free-running conditions without active mechanical conditioning. In such contexts, overheating risk is commonly quantified using

Table 1. Thermal properties of the building components: glazing type, external walls and roof

Element	Configuration	Glazing type	Solar Heat Gain Coefficient (SHGC)	Direct Solar Transmittance	U-Value [$W/m^2 \cdot K$]
Windows	0	Single Clear Glazing (6 mm)	0.819	0.775	5.778
	1	Double Glazing Low-E e=1 Tint 6/13/6	0.380	0.284	1.761

Element	Configuration	Layer type	Thickness (m)	Density (kg/m^3)	Thermal conductivity (w/m.k)	U-Value [$W/m^2 \cdot K$]
External wall configurations using EPS	0: Uninsulated wall and roof	Ciment mortar	0.015	2000	1.40	0.829
		Brick	0.200	743	0.197	
		Ciment mortar	0.015	2000	1.40	
	1: Insulated wall with eps 10 cm	Ciment mortar	0.015	2000	1.40	0.252
		Brick	0.070	743	0.197	
		EPS insulation	0.100	100	0.039	
		Air gap	0.020	1	0.117	
		Brick	0.120	743	0.197	
		Ciment mortar	0.015	2000	1.40	
Roof configurations using EPS	0: Uninsulated roof	Tiling	0.010	2100	1.50	1.598
		Slab	0.040	2400	1.70	
		Slope forme	0.050	600	0.42	
		Compression slab	0.050	2400	1.70	
		Slab	0.200	0.80	1300	
		Plaster	0.020	0.35	950	
	1: Insulated roof with eps 10 cm	Tiling	0.010	2100	1.50	0.287
		Slab	0.04	2400	1.70	
		EPS insulation Heavyweight	0.10	25	0.035	
		Slope forme	0.05	600	0.42	
		Compression slab	0.05	2400	1.70	
		Slab	0.2	0.8	1300	
		Plaster	0.02	0.35	950	
External wall configurations using PCM	1: Integration of BioPCM M27/Q29 (4 cm)	Ciment mortar	0.015	2000	1.40	1.645
		Brick	0.2	1920	0.72	
		BioPCM	0.04	235	0.20	
		Ciment mortar	0.015	2000	1.40	
Roof configurations using PCM	1: Integration of Bio-PCM M27/Q29 (4 cm)	Tiling	0.01	2100	1.50	1.211
		Slab	0.04	2400	1.70	
		Slope forme	0.05	600	0.42	
		Compression slab	0.05	2400	1.70	
		Slab	0.2	0.8	1300	
		BioPCM	0.04	235	0.20	
		Plaster	0.02	0.35	950	
		Slab	0.04	2400	1.70	

temperature-based threshold metrics expressed in hours of exceedance.

Temperature thresholds

To distinguish between moderate and severe discomfort conditions, fixed operative temperature thresholds were defined as follows:

- Extreme heating discomfort (EHD): Top < 16 °C
- Heating discomfort (HD): 16 °C ≤ Top < 18 C
- Cooling discomfort (CD): Top > 26 °C
- Extreme cooling discomfort (ECD): Top > 28 °C

The lower thresholds (16–18 °C) are consistent with minimum indoor temperature recommendations reported in EN 16798-1 and ASHRAE Standard 55 for acceptable thermal conditions in residential buildings.

The upper thresholds (26 °C and 28 °C) are aligned with commonly adopted over-heating risk criteria in residential building assessments and correspond to temperature levels frequently associated with moderate and severe overheating in free-running dwellings. In particular, temperatures exceeding 28 °C are often considered indicative of critical thermal stress in naturally ventilated residential spaces.

Rationale for fixed threshold approach

Although adaptive comfort models provide temperature limits that vary with outdoor conditions and are widely applied in free-running building assessment under changing climates (Delgado-Gutierrez et al., 2025; Tellache et al., 2025), fixed operative temperature thresholds were adopted in this study to:

- Ensure direct comparability across present and future climatic horizons;
- Enable consistent quantification of extreme overheating under climate change scenarios;

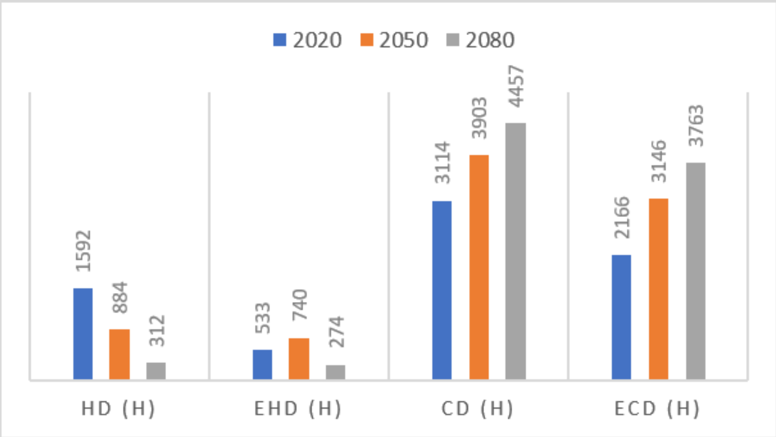

Figure 2. Evolution of HD, CD, EHD and ECD across climatic horizons of configuration (0-0-0) (Source: Authors' own elaboration)

- Provide clear identification of severe thermal stress conditions independent of adaptive assumptions.

This approach is particularly suitable for long-term climate resilience assessment, where the objective is to evaluate the robustness of envelope strategies under progressively intensifying thermal stress and to enable consistent comparison of overheating vulnerability across climatic horizons, as commonly adopted in recent studies investigating building thermal performance under future warming conditions (Amraoui et al., 2025; Flores-Larsen & Bre, 2026).

Derived indicators

Based on these thresholds, the following aggregated indicators were computed for each simulation case:

- Total Discomfort (TD): sum of heating and cooling discomfort hours;
- Extreme Total Discomfort (ETD): sum of extreme heating and extreme cooling discomfort hours.

Indicators were expressed both as Annual number of hours (h/year) and Percentage of total annual hours (%).

This dual representation enables both absolute and relative comparison of performance across envelope configurations, climatic horizons, infiltration levels, and spatial scales.

Simulation Matrix and Analysis Framework

The parametric framework developed in this study combines:

- Five envelope configurations (reference, insulation-only, glazing-only, PCM-only, combined strategy);
- Three infiltration levels (0, 1.5, and 2.2 ACH);
- Three climatic horizons (2020, 2050, 2080);
- Three spatial scales of analysis (building-level, bedroom, and living room).

This structured simulation matrix enables a systematic comparison of 135 passive strategy configurations conducted in two complementary stages:

- Baseline comparative analysis: In the first stage, a baseline scenario was defined by fixing infiltration at 1.5 ACH, representing typical and realistic airtightness con-ditions for residential buildings. This configuration made it possible to directly assess the individual and combined effects of the passive envelope strategies, as well as their evolution under current and future climates (2020, 2050, and 2080). In addition, it allowed a consistent comparison between building-level and room-level thermal responses.
- Airtightness sensitivity analysis

In the second stage, a sensitivity analysis was performed by varying infiltration rates (0, 1.5, and 2.2 ACH). This approach was used to evaluate how changes in airtightness influence the performance of each envelope configuration. It also made it possible to quantify the variation in thermal discomfort associated with air leakage, identify the most sensitive configurations, and assess their robustness under realistic construction variability.

This two-stage framework improves the clarity and reliability of the analysis, ensuring that the conclusions are not dependent on a single assumption regarding air exchange.

RESULTS

Overview of Thermal Discomfort Indicators

Unless otherwise specified, the results presented in Sections *Building-level thermal comfort performance* and *Room-level thermal comfort performance* correspond to the baseline infiltration scenario (1.5 ACH), representing moderate and realistic airtightness conditions. The influence of infiltration variability is analysed separately in Section *Sensitivity to infiltration and climate evolution* to assess robustness under envelope infiltration uncertainty.

Building-Level Thermal Comfort Performance

Climate-driven transition

Figure 2 illustrates the evolution of heating discomfort (HD), cooling discomfort (CD), and their extreme components EHD and ECD across climatic horizons.

Under 2020 climatic conditions, the reference building already exhibits a predominantly overheating-driven discomfort pattern. Total annual discomfort reaches 4706 h, with cooling discomfort representing 35.6% of annual hours and heating discomfort 18.2%. Extreme overheating already dominates, accounting for 69.6% of cooling discomfort.

Table 2. Building-level thermal discomfort indicators (hours and annual percentages) for all envelope configurations under the 2020 climate

Configuration	HD (h)	HD (%)	EHD (h)	EHD (%)	CD (h)	CD (%)	ECD (h)	ECD (%)	TD (h)	TD (%)	ETD (h)	ETD (%)
0-0-0	1592	18.2	533	6.1	3114	35.5	2166	24.7	4706	53.7	2699	30.8
1-0-0	1133	12.9	224	2.6	2921	33.3	1810	20.7	4054	46.3	2034	23.2
0-1-0	2168	24.7	925	10.6	2884	32.9	1789	20.4	5052	57.7	2714	31.0
0-0-1	1495	17.1	550	6.3	3312	37.8	2444	27.9	4807	54.9	2994	34.2
1-1-1	1793	20.5	597	6.8	2463	28.1	1333	15.2	4256	48.6	1930	22.0

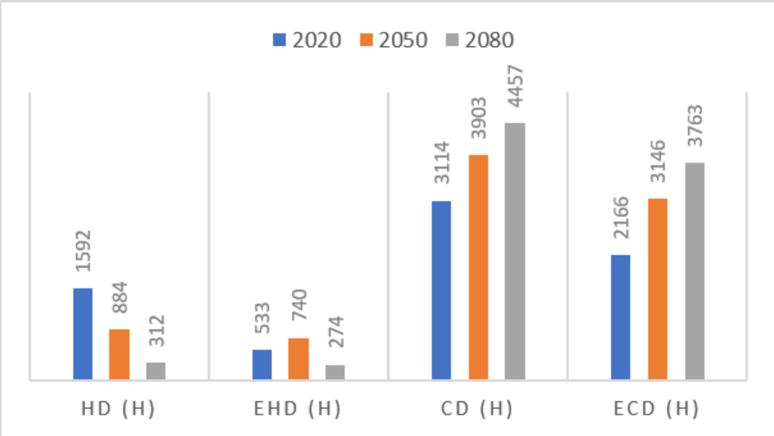

Figure 3. Comparative building-level discomfort indicators across all envelope configurations under the 2020 climate (Source: Authors' own elaboration)

Although overheating dominates, cold-related discomfort remains relevant, with extreme heating representing 6.1% of annual hours.

By 2050, heating discomfort decreases significantly (884 h), while cooling discomfort increases to 3903 h. Extreme overheating becomes predominant, representing more than 80.60% of cooling-related discomfort.

In 2080, overheating becomes the dominant thermal condition, with cooling discomfort reaching 4457 h and extreme overheating accounting for more than 84.43% of cooling exposure, while heating discomfort becomes marginal.

These results indicate a progressive shift toward a severity-dominated overheating regime under climate change.

Effect of envelope configurations

Table 2 and **Figure 3** compare building-level discomfort indicators across all envelope configurations under the 2020 climate. The results reveal pronounced seasonal trade-offs and highlight the importance of distinguishing between annual discomfort and its extreme components.

Configuration (1 0 0) reduces total discomfort to 4054 h, representing the lowest value among all single-strategy configurations. Both CD (2921 h) and HD (1133 h) and there extreme indicators decrease compared to the reference case, indicating an overall improvement in thermal stability.

In contrast, configuration (0 1 0) reduces overheating but significantly increases heating discomfort, leading to the highest total discomfort (5052 h).

Configuration (0 0 1) shows limited effectiveness, with increased overheating severity and higher total discomfort compared to the reference case.

The combined configuration (1 1 1) achieved the most balanced performance, with 4256 discomfort hours (48.6%) and the lowest proportion of extreme discomfort (22%). Overheating hours were reduced to 2463 h, ECD were significantly limited (1333 h), while HD remained moderate (597 h).

Configuration robustness under future climates (2050 and 2080)

Figure 4 and **Table 3** present the evolution of building-level thermal discomfort under future climate scenarios (2050 and 2080). Results indicate a progressive shift toward a severity-dominated overheating regime, where extreme discomfort becomes more significant than total discomfort.

Under the 2050 scenario, all configurations show a clear transition toward overheating dominance. Total discomfort remains high (4218–4979 h), with extreme overheating becoming the main contributor.

The insulation-only configuration (1–0–0) reduces total discomfort to 4218 h (−569 h compared to reference), mainly through reduced heating discomfort, while extreme overheating remains high (2827 h).

The PCM-only configuration (0–0–1) performs poorly, with the highest total dis-comfort (4979 h) and extreme overheating (3132 h), indicating increased exposure to high-temperature conditions.

The combined configuration (1–1–1) provides the most balanced performance, reducing total discomfort to 4370 h and extreme overheating to 2160 h (−986 h compared to reference), while maintaining low heating discomfort.

Overall, 2050 results highlight a transition toward an overheating-driven regime, dominated by extreme temperature conditions.

Table 3. Thermal discomfort indicators under future climate scenarios (hours and %)

Climate scenario	Configuration	HD (h)	HD (%)	EHD (h)	EHD (%)	CD (h)	CD (%)	ECD (h)	ECD (%)	TD (h)	TD (%)	ETD (h)	ETD (%)
2050 (RCP 8.5)	0-0-0	312	3.6	38	0.4	4457	50.9	3763	43.0	4769	54.4	3801	43.4
	1-0-0	71	0.8	0	0.0	4309	49.2	3485	39.8	4380	50.0	3485	39.8
	0-1-0	548	6.3	63	0.7	4204	48.0	3462	39.5	4752	54.2	3525	40.2
	0-0-1	520	5.9	88	1.0	4452	50.8	3725	42.5	4972	56.8	3813	43.5
	1-1-1	276	3.6	27	0.3	3972	45.3	3005	34.3	4248	48.5	3032	34.6
2080 (RCP 8.5)	0-0-0	312	3.6	38	0.4	4457	50.9	3763	43.0	4769	54,4	3801	43,4
	1-0-0	411	4.7	29	0.3	3807	43.5	2827	32.3	4218	48.1	2856	32.6
	0-1-0	1267	14.5	341	3.9	3676	42.0	2826	32.3	4943	56.4	3167	36.1
	0-0-1	1080	12.3	297	3.4	3899	44.5	3132	35.8	4979	56.8	3429	39.1
	1-1-1	920	10.5	143	1.6	3450	39.4	2160	24.7	4370	49.9	2303	26.3

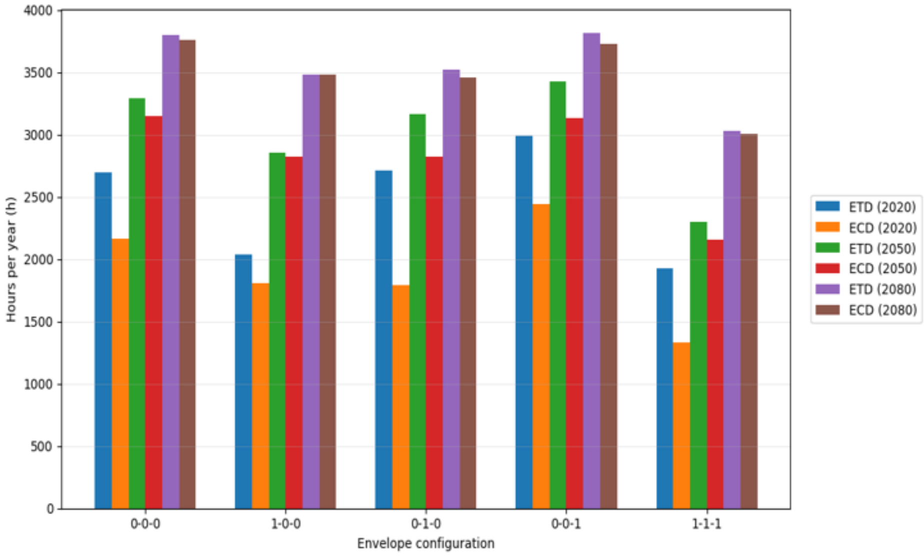

Figure 4. ECD and ETD across configurations and years (2020, 2050 and 2080) (Source: Authors' own elaboration)

Table 4. Building, bedroom and living room-level thermal discomfort hours under the 2020 climate (1.5 ACH)

Scale	HD (h)	EHD (h)	CD (h)	ECD (h)	TD (h)	ETD (h)
Building	1592	533	3114	2166	4706	2699
Bedroom	852	271	3629	2849	4481	3120
Living Room	897	274	3773	2928	4670	3202

Under the 2080 scenario, thermal conditions become almost entirely dominated by overheating, while cold-related discomfort becomes negligible.

The reference configuration records 4769 h of total discomfort, with extreme over-heating reaching 3763 h (43.4% of annual hours).

The insulation-only configuration reduces total discomfort to 4380 h, but extreme overheating remains high (3485 h). Heating discomfort is nearly eliminated.

The glazing-only configuration shows limited improvement, with total discomfort similar to the reference case.

The PCM-only configuration again performs worst, with the highest total discomfort (4972 h) and extreme overheating (3725 h).

The combined configuration (1–1–1) achieves the best performance, reducing total discomfort to 4248 h and extreme overheating to 3005 h, although overheating remains dominant.

Overall, the 2080 scenario confirms a fully overheating-driven regime, where extreme high-temperature exposure governs building thermal performance.

Room-Level Thermal Comfort Performance

Reference configuration

Under the reference configuration (0–0–0) in 2020, room-level results reveal substantially higher overheating exposure than building-level indicators (See **Table 4**, and **Figure 5**). Extreme cooling discomfort (ECD) increases from 2166 h at building level to 2849 h in the bedroom and 2928 h in the living room, corresponding to amplification factors of 1.32 and 1.35, respectively. Cooling discomfort (CD) exceeds 3600 h in both rooms, remaining substantially higher than the building-level value (3114 h). In contrast, heating discomfort is lower at room scale than in aggregated building results. These findings highlight strong spatial heterogeneity and suggest that building-level indicators underestimate overheating in exposed rooms.

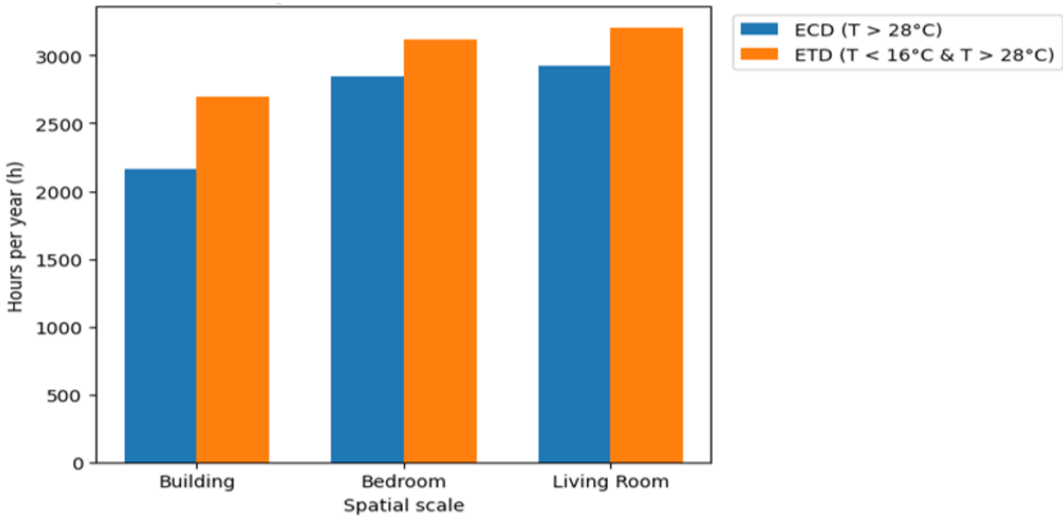

Figure 5. Comparison of ECD and ETD at building and room scales (2020) (Source: Authors' own elaboration)

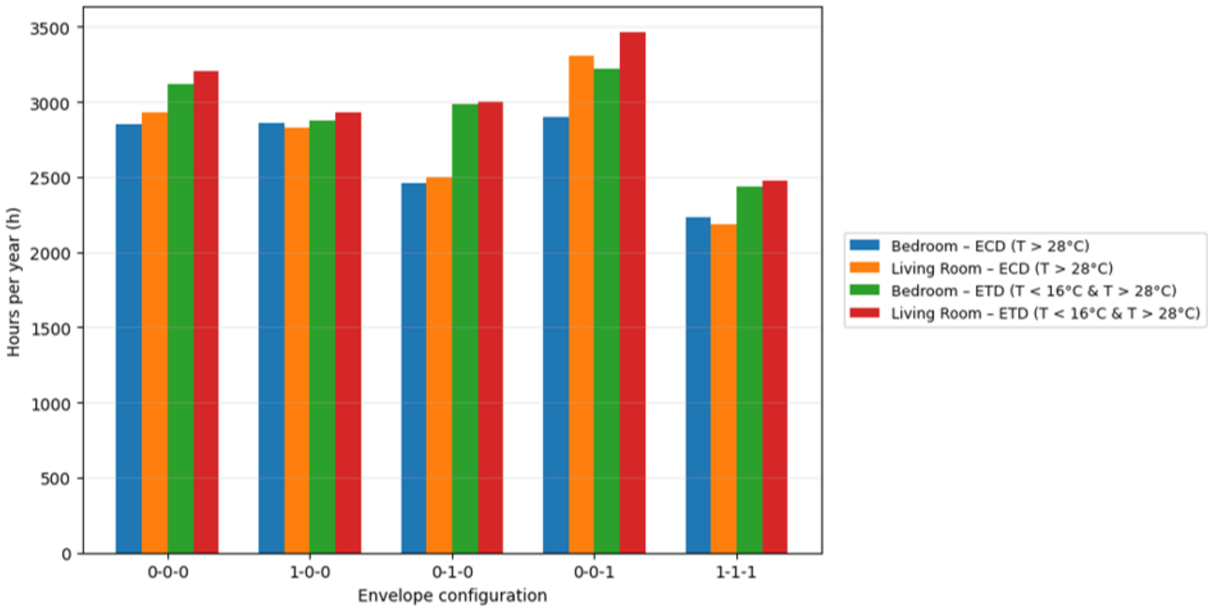

Figure 6. Room-level comparison of ECD and ETD across configurations (2020, 1.5 ACH) (Source: Authors' own elaboration)

Differential response of configurations

Envelope strategies show differentiated performance at room level, with amplified seasonal trade-offs. The insulation-only configuration (1–0–0) significantly improves heating conditions, with heating discomfort decreasing from 852 h to 305 h in the bedroom and from 897 h to 480 h in the living room. However, its impact on overheating remains limited, with only marginal reductions in extreme cooling discomfort (≈-20 to -50 h).

The glazing-only configuration (0–1–0) reduces extreme overheating more effectively, with ECD decreasing by 389 h in the bedroom and 425 h in the living room. However, this improvement is offset by a substantial increase in heating discomfort, rising by +608 h in the bedroom and +483 h in the living room, highlighting a strong seasonal trade-off.

The PCM-only configuration (0–0–1) shows limited or adverse performance. In the bedroom, extreme cooling increases slightly (+68 h), while in the living room it rises significantly from 2928 h to 3307 h (+379 h), indicating increased exposure to over-heating.

The combined configuration (1–1–1) provides the best overall performance. Extreme cooling discomfort decreases by 620 h in the bedroom and 746 h in the living room, while extreme total discomfort is reduced by up to 730 h. Consequently, the share of extreme discomfort decreases from 35.6% to 27.9% in the bedroom and from 36.6% to 28.2% in the living room. This improvement is accompanied by a moderate increase in heating discomfort (+49 h and +140 h, respectively).

As illustrated in **Figure 6** and **Table 5**, Room-level results confirm higher sensitivity to envelope strategies and demonstrate that combined solutions are the most effective in reducing extreme overheating in thermally exposed spaces.

Table 5. Bedroom (A) and Living Room (B) thermal discomfort indicators under the 2020 climate (infiltration 1.5 ACH): full indicators (%) across envelope configurations and differences relative to the reference case (0–0–0)

A: Bedroom

Configuration	HD (%)	EHD (%)	CD (%)	ECD (%)	TD (%)	ETD (%)	ΔHD (%)	ΔEHD (%)	ΔCD (%)	ΔECD (%)	ΔTD (%)	ΔETD (%)
0-0-0	9.7	3.1	41.4	32.5	51.2	35.6	+0.0	+0.0	+0.0	+0.0	+0.0	+0.0
1-0-0	3.5	0.2	44.2	32.6	47.7	32.8	−6.2	−2.9	+2.8	+0.1	−3.5	−2.8
0-1-0	16.7	6.0	37.7	28.1	54.3	34.1	+7.0	+2.9	−3.7	−4.4	+3.1	−1.5
0-0-1	11.0	4.0	42.0	33.0	53.0	37.0	+1.3	+0.9	+0.6	+0.5	+1.8	+1.4
1-1-1	10.3	2.4	37.1	24.9	47.4	27.9	+0.6	−0.7	−4.3	−7.6	−3.8	−7.7

B: Living room

Configuration	HD (%)	EHD (%)	CD (%)	ECD (%)	TD (%)	ETD (%)	ΔHD (%)	ΔEHD (%)	ΔCD (%)	ΔECD (%)	ΔTD (%)	ΔETD (%)
0-0-0	10.2	3.1	43.1	33.4	53.3	36.6	+0.0	+0.0	+0.0	+0.0	+0.0	+0.0
1-0-0	5.5	1.1	43.4	32.3	48.9	33.4	−4.7	−2.0	+0.3	−1.1	−4.4	−3.2
0-1-0	15.8	5.7	37.8	28.6	53.6	34.3	+5.6	+2.6	−5.3	−4.8	+0.3	−2.3
0-0-1	7.0	2.0	48.0	38.0	54.0	40.0	−3.2	−1.1	+4.9	+4.6	+0.7	+3.4
1-1-1	11.8	3.3	36.1	24.9	48.0	28.2	+1.6	+0.2	−7.0	−8.5	−5.3	−8.4

Table 6. Relative variation (%) of discomfort indicators with infiltration change (reference: 1.5 ACH)

Configuration	CD 1.5→0	CD 1.5→2.2	ECD 1.5→0	ECD 1.5→2.2	HD 1.5→0	HD 1.5→2.2	EHD 1.5→0	EHD 1.5→2.2
0-0-0	+10.6	−5.2	+40.5	−8.9	−73.5	+28.9	−93.3	+70.0
0-0-1	+1.5	−0.8	+17.1	−4.5	−37.8	+10.6	−58.4	+18.9
0-1-0	+5.6	−7.5	+53.9	−8.1	−66.0	+12.6	−90.1	+36.9
1-0-0	+39.6	−9.1	+77.6	−13.5	−100.0	+53.6	−100.0	+168.8
1-1-1	+39.1	−8.7	+89.0	−9.4	−100.0	+33.2	−100.0	+71.5

Temporal divergence between building and room scales under climate change

Climate change increases not only the magnitude of thermal discomfort but also the divergence between building- and room-level behaviour.

At the building scale, extreme cooling discomfort (ECD) rises from 2166 h in 2020 to 3146 h in 2050 and 3763 h in 2080, indicating a shift toward a severity-dominated overheating regime. At room level, this transition occurs earlier and more intensely. In 2020, the bedroom already reaches 2849 h (+31,5%) and the living room 2928 h (+35.2%) compared to the building average.

By 2050, ECD exceeds 3400 h/year in both rooms, approaching late-century building-level values. At this stage, extreme overheating becomes dominant at room scale, while a similar regime appears later at building scale. By 2080, ECD exceeds 3900 h in both rooms, confirming a widening gap between scales.

The living room follows a similar but slightly attenuated trend, likely due to its larger volume and higher thermal inertia.

The results reveals that thermally exposed rooms transition earlier to a severity-dominated regime, indicating that building-level indicators increasingly underestimate localized overheating under future climate conditions.

Building-level sensitivity to infiltration

Table 6 quantifies the variation of CD, HD, and their extreme values relative to the reference infiltration (1.5 ACH), while **Figure 7** illustrates the corresponding sensitivity patterns.

A clear asymmetry is observed between infiltration reduction (1.5 → 0 ACH) and increase (1.5 → 2.2 ACH).

For cooling-related indicators, reducing infiltration systematically increases discomfort. CD rises by +1.6% to +39.6%, while ECD shows stronger amplification, reaching +89.0% (1–1–1) and +77.9% (1–0–0). In contrast, increasing infiltration reduces CD (−5.2% to −9.1%) and ECD (−4.5% to −13.5%), indicating that infiltration contributes to passive cooling under current conditions.

Heating-related indicators exhibit the opposite trend. Reducing infiltration significantly decreases HD (−37.8% to −100%) and EHD (−58.4% to −100%). Conversely, increasing infiltration leads to higher heating discomfort, with HD increasing by +10.6% to +53.6% and EHD reaching up to +168.8% (1–0–0).

Extreme indicators (ECD and EHD) show greater sensitivity than total indicators, highlighting the nonlinear response of peak thermal conditions.

Table 6 quantifies the variation of CD, HD, and their extreme values relative to the reference infiltration (1.5 ACH), while **Figure 7** illustrates the corresponding sensitivity patterns.

A clear asymmetry is observed between infiltration reduction (1.5 → 0 ACH) and increase (1.5 → 2.2 ACH).

For cooling-related indicators, reducing infiltration systematically increases discomfort. CD rises by +1.6% to +39.6%, while ECD shows stronger amplification, reaching +89.0% (1–1–1) and +77.9% (1–0–0). In contrast, increasing infiltration reduces CD (−5.2% to −9.1%) and ECD (−4.5% to −13.5%), indicating that infiltration contributes to passive cooling under current conditions.

Heating-related indicators exhibit the opposite trend. Reducing infiltration significantly decreases HD (−37.8% to −100%) and EHD (−58.4% to −100%). Conversely, increasing infiltration leads to higher heating discomfort, with HD increasing by +10.6% to +53.6% and EHD reaching up to +168.8% (1–0–0).

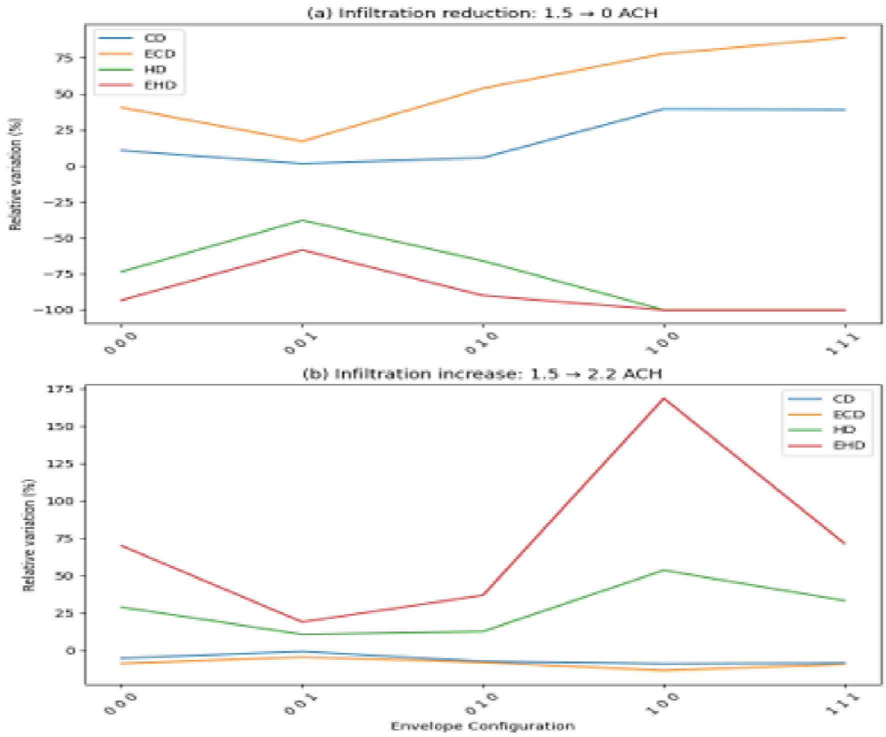

Figure 7. Relative variation (%) of CD, ECD, HD and EHD under 2020 climate conditions: (a) infiltration reduction from 1.5 ACH to 0 ACH; (b) infiltration increase from 1.5 ACH to 2.2 ACH (Source: Authors' own elaboration)

Table 7. Absolute variations in cooling and heating discomfort indicators due to infiltration changes (1.5 → 0 ACH and 1.5 → 2.2 ACH) across envelope configurations under 2020, 2050 and 2080 climate scenarios

Climate scénario	Configuration	CD (h) 1.5→0	ECD (h) 1.5→0)	HD (h) 1.5→0	EHD (h) 1.5→0	CD (h) 1.5→2.2	ECD (h) 1.5→2.2	HD (h) 1.5→2.2	EHD (h) 1.5→2.2
2020	0 0 0	432	878	-1170	-497	-213	-193	460	373
	0 0 1	66	418	-565	-321	-33	-111	159	104
	0 1 0	224	964	-1430	-833	-297	-145	274	341
	1 0 0	1595	1409	-1133	-224	-365	-245	607	378
	1 1 1	1404	1186	-1793	-597	-311	-125	596	427
2050 RCP8.5	0 0 0	711	639	-815	-144	-125	-199	268	124
	0 0 1	158	298	-419	-207	-45	-179	196	148
	0 1 0	393	229	-1211	-341	-27	-269	288	230
	1 0 0	2366	1224	-411	-29	-154	-286	463	138
	1 1 1	700	1314	-920	-143	-279	-177	461	259
2080 RCP8.5	0 0 0	1104	540	-308	-38	-140	-210	216	42
	0 0 1	639	437	-468	-88	-26	-202	169	53
	0 1 0	75	181	-290	-49	-58	-190	279	79
	1 0 0	3428	1184	-71	0	-134	-258	198	28
	1 1 1	1957	939	-276	-27	-384	-1352	641	107

Extreme indicators (ECD and EHD) show greater sensitivity than total indicators, highlighting the nonlinear response of peak thermal conditions.

Temporal evolution under climate change and varying infiltration

The temporal sensitivity to infiltration was analysed for all configurations under 2020, 2050, and 2080 climates. Relative variations of cooling (CD, ECD) and heating (HD, EHD) discomfort were evaluated for infiltration reduction (1.5 → 0 ACH) and increase (1.5 → 2.2 ACH) (See **Table 7**, **Figure 8**].

Response to infiltration reduction (1.5 → 0 ACH)

Cooling Response (CD and ECD): Reducing infiltration increases cooling discomfort across all configurations, with sensitivity intensifying toward 2080. CD rises most strongly in configuration 1–0–0, from +39.6% (2020) to +66.8% (2080), followed by 1–1–1, while 0–0–1 remains minimally affected (≲ +3.4%). ECD follows the same trend but with higher magnitudes, reaching +89.0% (1–1–1) and +77.9% (1–0–0) in 2020. Although amplification decreases in later periods, 1–0–0 remains the most sensitive (+60.8% in 2050; +34.0% in 2080).

Heating Response (HD and EHD): In contrast, heating discomfort decreases significantly. HD is fully suppressed (−100%) in configurations 1–0–0 and 1–1–1 across several periods, while 0–0–1 shows smaller reductions (−37.8% in 2020; −52.9% in 2080). EHD follows a similar pattern, with reductions reaching −100% in the most sensitive configurations.

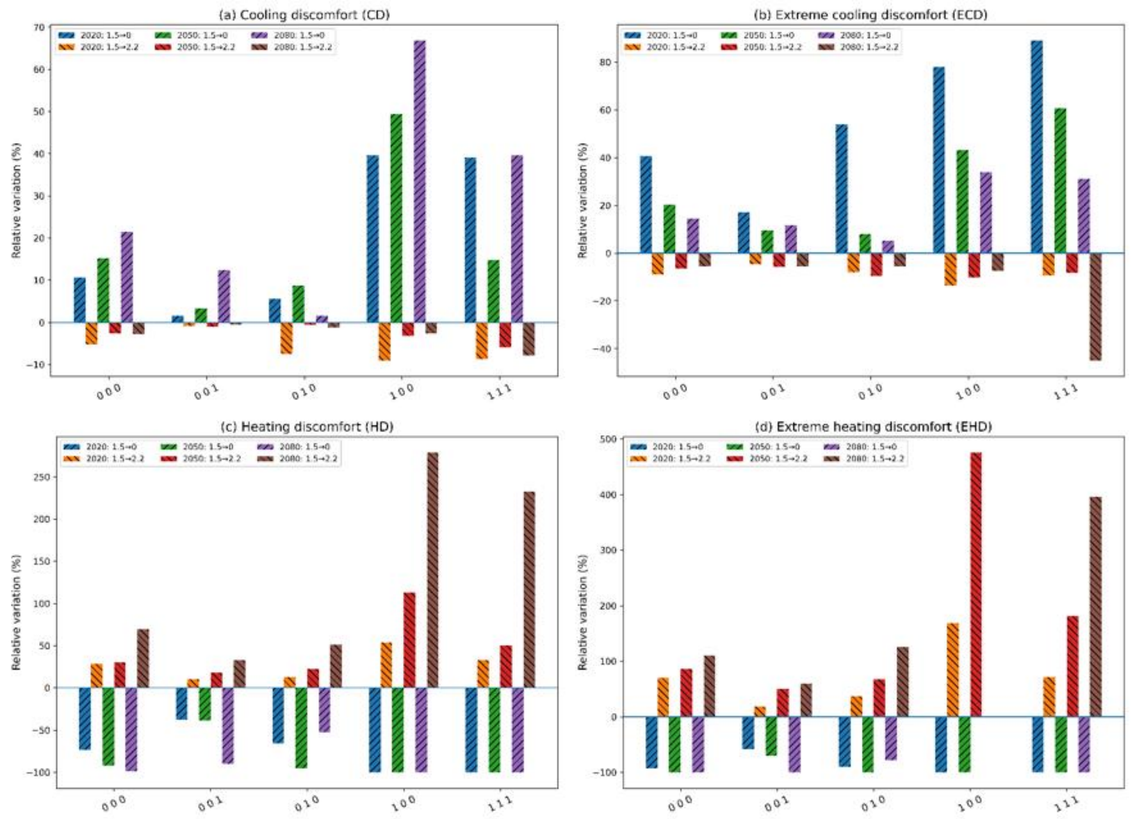

Figure 8. Temporal sensitivity of thermal discomfort indicators to infiltration changes under current and future climates (Source: Authors' own elaboration)

Response to infiltration increase (1.5 → 2.2 ACH)

Cooling Response (CD and ECD): In contrast, heating discomfort decreases significantly. HD is fully suppressed (−100%) in configurations 1–0–0 and 1–1–1 across several periods, while 0–0–1 shows smaller reductions (−37.8% in 2020; −52.9% in 2080). EHD follows a similar pattern, with reductions reaching −100% in the most sensitive configurations.

Heating Response (HD and EHD): Heating discomfort increases substantially with infiltration. HD rises from +53.6% (2020) to +278.9% (2080) in configuration 1–0–0, while 0–0–1 remains the least sensitive. EHD shows the highest amplification, exceeding +475% in 2050 and re-maining above +300% in 2080.

Room-level sensitivity to infiltration under climate conditions

Room-level discomfort metrics show a consistent bidirectional response to infiltration changes across 2020, 2050 (RCP8.5), and 2080 (RCP8.5). Two contrasting effects are observed when infiltration is reduced (1.5→0 ACH) versus increased (1.5→2.2 ACH), with configuration and climate-dependent magnitudes. The quantitative variations for both directions (1.5→0 and 1.5→2.2 ACH) are summarised in **Figure 9**.

- **Infiltration reduction (1.5→0 ACH):** heating improvement with concur-rent overheating amplification.

Across both rooms and all periods, decreasing infiltration from 1.5 to 0 ACH reduces heating discomfort and extreme heating discomfort, while increasing cooling discomfort and extreme cooling discomfort. Under 2020 conditions, the strongest room-level increases in cooling exposure under tightening occur in insulation-dominated configurations. For configuration 1–0–0, ΔCD (1.5→0) reaches +2330 h in the bedroom and +2512 h in the living room, while ΔECD (1.5→0) reaches +1863 h (bedroom) and +1892 h (living room). The combined configuration 1–1–1 also exhibits substantial increases (e.g., bedroom ΔCD = +1603 h, ΔECD = +1306 h).

- **Infiltration increase (1.5→2.2 ACH):** heating amplification with partial mitigation of overheating.

Increasing infiltration from 1.5 to 2.2 ACH produces the opposite pattern. Heating discomfort increases in both rooms (ΔHD > 0; ΔEHD > 0), while cooling discomfort decreases (ΔCD < 0; ΔECD < 0). In 2020, the largest heating amplification is observed in configuration 1–1–1, with ΔHD (1.5→2.2) of +529 h in the bedroom and +495 h in the living room. Cooling discomfort decreases simultaneously, with reductions reaching −350 h (bedroom, 1–0–0) and −416 h (living room, 1–0–0); extreme cooling decreases by −332 h (bedroom, 1–0–0) and −305 h (living room, 1–0–0).

- **Temporal evolution (2020→2050→2080):** attenuation of heating sensitivity and escalation of cooling exposure.

From 2020 to 2080, heating-related deltas systematically decrease in magnitude, while the cooling-related deltas associated with infiltration tightening remain high in insulation-dominated configurations. For example, in the bedroom, ΔHD (1.5→2.2) de-creases from +333 h (2020, 0–0–0) to +187 h (2050) and becomes much smaller by 2080. Conversely, tightening-driven overheating amplification remains pronounced for 1–0–0, with ΔCD (1.5→0) of +2567 h

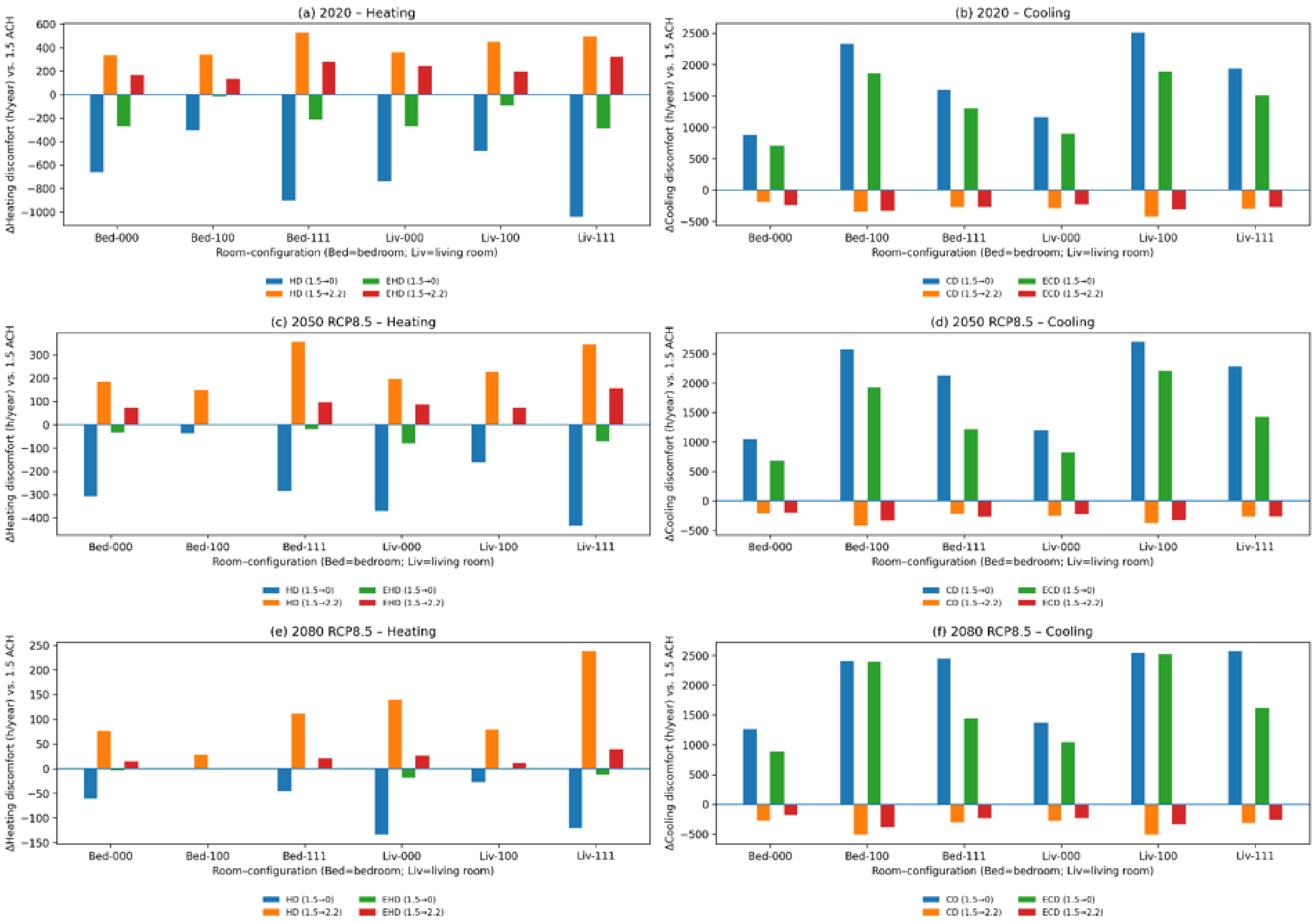

Figure 9. Absolute variations in room-level heating (HD, EHD) and cooling (CD, ECD) discomfort hours relative to the 1.5 ACH baseline under present and future climates (Source: Authors' own elaboration)

(2050) and still very high under 2080 conditions. Similar patterns are observed in the living room as illustrated in **Figure 9(a)**.

Overall, the room-level results identify infiltration as a strong seasonal trade-off driver: tightening (1.5→0) systematically reduces heating exposure while amplifying cooling exposure, whereas loosening (1.5→2.2) systematically amplifies heating exposure while reducing cooling exposure. These effects are strongest in insulation-intensive configurations (1–0–0 and 1–1–1) and evolve across climatic horizons.

DISCUSSION

Climate Warming and the Shift Toward Severity-Dominated Discomfort

The results obtained indicate a marked change in indoor thermal conditions as a result of ongoing climate warming. Between 2020 and 2080 (RCP 8.5), overheating episodes not only become more frequent but also more intense, leading to a noticeable change in the nature of thermal discomfort, notably discomfort due to ECD, which has gradually become the dominant factor.

This trend is consistent with projections for the Mediterranean and North African regions, identified as areas sensitive to climate change (IPCC, 2021; Spinoni et al., 2020), where by the end of the century, average temperatures and night-time lows are expected to rise significantly, alongside more frequent and prolonged heatwaves. Warmer nights are particularly critical, as they reduce building's ability to dissipate the heat accumulated during the day.

Another factor is that successive heatwaves, along with reduced temperature differences between indoors and outdoors, limit heat dissipation. Consequently, heat accumulates within the building envelope over several consecutive days, leading to higher indoor temperature peaks and longer periods of discomfort.

projecting into the year 2080, the trend suggests that heat stress will become a persistent phenomenon, characterised by increased severity. This suggests that future discomfort will be linked more to extreme conditions than to average temperature variations.

Similar trends have been reported in recent overheating resilience studies in Europe and hot climates (Driouech et al., 2020; Younes et al., 2011), yet the present study extends this understanding by demonstrating a progressive inversion in the internal structure of discomfort: extreme thresholds become the dominant contributor to annual thermal exposure.

The analysis across 2020, 2050, and 2080 under the RCP 8.5 scenario provides insight into how envelope strategies evolve under increasing climatic pressure. Rather than evaluating a single future projection, the study captures the trajectory of parameter performance degradation or robustness over time, thereby aligning with long-term adaptation planning frameworks.

Thermophysical Mechanisms and Parameter Interactions

The behaviour of insulation, glazing, PCM, and infiltration highlights that passive strategies operate through interacting conductive, radiative, and latent heat transfer mechanisms, whose relative influence evolves under climate change.

Insulation: winter stabilization versus summer heat retention

Thermal insulation reduces conductive heat transfer by lowering U-values and limiting heat exchange between indoor and outdoor environments. Under 2020 conditions, where overheating already dominates, insulation primarily improves winter performance by reducing heating-related discomfort, while its impact on summer overheating remains limited.

Under RCP 8.5 warming, elevated ambient and night-time temperatures reduce the thermal gradient required for passive heat dissipation. As diurnal temperature amplitude decreases, the building envelope shifts from a cyclic heat-exchange regime toward a heat accumulation behaviour. In this context, insulation not only limits heat gains but also restricts heat release, reducing the envelope's discharge capacity.

As a result, insulation alone does not effectively mitigate extreme overheating under 2050 and 2080 conditions. While winter stabilization remains significant, its contribution to thermal resilience becomes increasingly constrained. These findings support previous studies highlighting heat entrapment risks in highly insulated buildings under climate change (Fosas et al., 2018).

Glazing: Solar gain control as peak temperature regulator

High-performance glazing modifies the building's radiative heat balance by reducing short-wave solar gains through lower solar heat gain coefficients (SHGC) and improved thermal transmittance. In hot, semi-arid climates, where solar radiation is a dominant factor in summer heat gain, the use of high-performance glazing designed to limit solar gain becomes a key factor in reducing indoor temperature peaks. This be-haviour is particularly noticeable in rooms facing west and south, which are most exposed to solar gain, especially in the late afternoon.

The results indicate that controlling solar gain is more effective at reducing the maximum intensity of overheating than at reducing the overall duration of discomfort.

However, the thermal performance of rooms in winter is also affected when the type of glazing is modified. Indeed, passive heating in winter could be limited when using glazing that restricts solar gain, leading to increased thermal heatind dicscomfort. This trade-off highlights importance of evaluating glazing performance across the full annual energy balance, rather than focusing on a single perspective. Furthermore, as global warming intensifies, overheating makes glazing a key factor in mitigating in-ternal thermal stress.

The observed room-level amplification supports previous findings on orientation-sensitive overheating (Abanda & Byers, 2016), while extending them by showing that the effectiveness of solar control strategies increases with climate intensity. This highlights glazing design as a key parameter for thermal resilience in hot arid residential buildings.

PCM: Latent heat buffering under climatic constraints

PCM are intended to enhance thermal inertia through latent heat storage within a defined phase-transition range, reducing peak indoor temperatures by absorbing and releasing heat during melting and solidification cycles.

However, under 2020 conditions, the selected PCM, despite thermo-physical properties suited to the Marrakech climate (Salihi et al., 2024), does not significantly reduce cooling or extreme cooling discomfort. In some configurations, overheating slightly increases, indicating limited or suboptimal activation of latent heat storage.

This behaviour is primarily driven by climatic constraints. Elevated night-time temperatures limit complete solidification, reducing daily regeneration capacity. In addition, the absence of mechanical cooling and the controlled ventilation strategy restrict heat dissipation, leading to incomplete phase transitions and a mismatch between PCM transition temperature and indoor conditions.

As a result, PCM effectiveness is strongly dependent on diurnal temperature amplitude and night-time cooling potential, which are limited in hot arid climates.

Under 2050 and 2080 scenarios, PCM performance further deteriorates. Higher night-time temperatures reduce the thermal gradient required for full regeneration, while decreased diurnal amplitude leads to persistent partial melting. Consequently, the PCM layer loses its capacity to buffer peak temperatures, and extreme overheating remains high.

These findings confirm that PCM performance is highly climate-dependent and becomes increasingly constrained under future warming conditions, particularly in hot arid environments.

Combined strategy: Non-linear synergy

The (1–1–1) combined configuration proves that passive envelope design strategies have an interdependent effect. When insulation, glazing and PCM are used in combination, they each influence heat transfer in distinct yet interrelated ways, which alters the overall thermal behaviour of the building.

Compared to single-strategy cases, where individual parameters mainly affect a single physical process, the combined approach acts simultaneously on multiple mechanisms. Insulation reduces heat transfer through the building envelope, glazing limits solar gain, and PCM modulates the manner in which heat is stored and dissipated. As a result of these interactions, the overall response is not simply additive, as the impact of each component depends on the presence of the others, leading to a greater reduction in extreme overheating than when the strategies are applied separately.

The simulation carried out as part of this study shows that future climatic conditions will limit these performance levels, during which extreme thermal discomfort will remain a significant issue.

Airtightness and Infiltration as Climate-Dependent Drivers of Envelope Performance

The infiltration analysis (1.5→0 ACH and 1.5→2.2 ACH) reveals that this parameter is a structurally fundamental factor governing both winter heat loss and summer heat gain. Its impact depends on the configuration of the building envelope, the properties of the materials and climate change in the 2020, 2050 and 2080 scenarios.

Winter behaviour: Convective heat loss as a dominant mechanism

When air infiltration is reduced, thermal discomfort decreases significantly across all configurations, reaching −1793 hours in the combined configuration (1–1–1) under 2020 conditions. Conversely, an increase in air leakage leads to a substantial rise in cold discomfort, reaching up to +607 h (2020, 1–0–0) and +641 h (2080, 1–1–1).

These results confirm that air leakage is a major source of heat loss through convection in buildings. As the insulation of the building envelope increases, the relative im-portance of heat transfer by convection becomes more pronounced, which explains the higher sensitivity observed in the insulated configurations (1–0–0 and 1–1–1), in line with previous studies (Ascione et al., 2014).

Cooling behaviour: Heat retention, thermal inertia, and convective moderation

A reduction in cooling-related discomfort (up to −365 hours in 2020) was observed as the rate of air infiltration increased. This phenomenon highlights the role of convective heat exchange between the interior of the building and its surroundings in the dissipation of internal heat gains. This indicates that the cooling response exhibits clear asymmetry.

Furthermore, when air infiltration is reduced, cooling-related discomfort increases substantially, reaching +1595 hours in 2020 and +3428 hours in 2080 (1–0–0). This behaviour results from a reduced capacity for heat dissipation, particularly in insulated building envelopes with high thermal mass.

Another parameter influencing heat exchange and passive heat dissipation is the nocturnal temperature gradient, which either promotes or further limits passive heat dissipation depending on this gradient. To this end, in climatic conditions characterised by a rise in external temperature, the restriction of air exchange that characterises airtight configurations, alongside the limited thermal gradient, intensifies heat retention, prolonging the duration of overheating.

Interaction with envelope materials and thermal storage

The configurations analysed highlight how air infiltration interacts with the properties of the building envelope materials to influence the building’s thermal performance. It has been observed that these parameters act in a dependent manner and influence the observed behaviour.

Insulating the building envelope reduces heat transfer by conduction, thus limiting heat loss and gain through the building envelope while increasing the building’s dependence on heat exchange by convection, which makes air circulation all the more important for heat dissipation.

High-performance glazing acts as the key factor in controlling solar heat gain, by reducing the amount of heat entering the building. However, when combined with air infiltration, which causes significant heat exchange, the role of the glazing fails to offset the associated heat losses, thereby masking its effectiveness. Meanwhile, the integration of PCM, designed to improve the building’s ability to store and release heat, thereby helping to stabilise the building’s internal thermal conditions, is also affected by day-night temperature gradients, which impact their efficiency.

The (1–1–1) configuration exhibits a more pronounced effect in terms of parameter interaction, which, on the one hand, results in increased discomfort due to cooling, as air infiltration is reduced because heat is retention inside a highly insulated envelope with high thermal mass. On the other hand, higher infiltration rates facilitate heat dissipation in summer, thereby causing greater heat loss in winter, which increases heating-related discomfort.

The (1 1 1) configuration exhibits a more pronounced effect in terms of parameter interaction, which, on the one hand, results in increased discomfort due to cooling, as air infiltration is reduced because heat is retention inside a highly insulated envelope with high thermal mass. On the other hand, higher infiltration rates facilitate heat dissipation in summer, thereby causing greater heat loss in winter, which increases heating-related discomfort.

Overall, these finding confirm that the components of the building envelope interact in a non-linear manner, with each parameter having a variable weight depending on the other interacting parameters of the envelope.

Climate escalation and seasonal rebalancing

A comparison of the scenarios for the periods 2020, 2050 and 2080 highlights a gradual shift in seasonal weighting. Winter discomfort decreases in absolute terms in the warming scenarios, thereby reducing the quantitative impact of the decline in infiltration. Conversely, discomfort linked to cooling increases, and the amplification associated with reduced infiltration becomes more pronounced in end-of-century projections.

This temporal evolution suggests that global warming alters the seasonal weighting of infiltration effects rather than eliminating them. Convective exchange remains a structurally influential mechanism, but its dominant season of impact is gradually shifting towards summer overheating dynamics in the RCP8.5 trajectories (Ascione et al., 2014; IPCC, 2021).

Room-Level Amplification of Infiltration Effects Under Climate Escalation

Analyses conducted at the room level reveal an amplification of infiltration effects compared to the building-wide scale, demonstrating the importance of spatial resolution in assessing thermal performance. The bedroom and living room exhibit greater sensitivity due to their layout, which was smoothed out during the building-scale analysis, particularly in the case of highly insulated building envelopes

Reducing air infiltration decreases thermal discomfort related to heating but significantly amplifies discomfort related to cooling at the room scale, particularly in the 1–0–0 configuration. The presence of glazing, combined with high insulation and minimal air exchange, promotes heat retention and limits the dissipation of sensible heat, causing localized overheating. The results obtained deepen this understanding by demonstrating that this amplification is spatially heterogeneous and becomes more pronounced under future climate projections.

Conversely, increased air leakage (1.5→2.2 ACH) mitigates cooling discomfort while generating heating penalties that are more pronounced at the room scale, reflecting reduced thermal buffering capacity and higher sensitivity to convective heat transfer in small volumes. This highlights that infiltration acts as a localized convective driver rather than a purely envelope-level parameter.

Temporal evolution (2020→2050→2080) indicates a shift from winter-dominant sensitivity toward cooling-dominant vulnerability. Under warming scenarios consistent with high-emission pathways, the relative weight of heating discomfort decreases, while overheating amplification under airtight conditions remains substantial. Extreme cooling discomfort (ECD) shows sharper responsiveness than moderate indicators, highlighting threshold-sensitive behaviour and non-linear amplification of peak exposure.

Methodologically, this room-scale quantification represents a central contribution of the study. By demonstrating that building-level averages underestimate localized thermal stress-particularly in sleeping spaces-the results emphasize the necessity of spatially resolved modelling for long-term envelope optimisation in hot arid climates.

CONCLUSIONS

This study evaluated the long-term thermal comfort performance of a representative residential building in Marrakech under present and future RCP 8.5 climate conditions, considering envelope strategies, infiltration variability, and spatial scale effects.

The results reveal a progressive shift in indoor thermal stress under climate change. While heating-related discomfort decreases over time, cooling-related discomfort becomes increasingly dominant, leading to a transition toward a severity-dominated thermal regime by the end of the century. This evolution highlights the growing challenge of maintaining acceptable indoor conditions in hot semi-arid climates through passive measures alone.

Among individual strategies, insulation significantly reduces winter discomfort but provides limited mitigation of extreme overheating under future climates due to restricted heat dissipation. High-performance glazing effectively reduces peak over-heating in solar-exposed spaces, confirming the dominant role of solar gains, although it introduces winter penalties. PCM integration shows limited effectiveness under elevated night-time temperatures, highlighting its strong dependence on climatic conditions.

The combined strategy (insulation, glazing, and PCM) provides the most balanced performance, demonstrating a non-linear interaction between conductive, radiative, and storage mechanisms. However, even this integrated approach cannot fully offset overheating under late-century climate conditions.

Infiltration is identified as a key bidirectional driver. Reduced air exchange improves winter conditions but exacerbates summer overheating, particularly in highly insulated envelopes. Under climate change, this effect shifts toward a cooling-dominated vulnerability.

Furthermore, room-level analysis reveals that building-averaged indicators systematically underestimate extreme overheating. Solar-exposed rooms, particularly west- and south-oriented spaces, experience earlier and more intense transitions toward severity-dominated conditions.

These findings demonstrate that climate-resilient design in hot arid regions requires integrated envelope strategies, controlled airtightness, and room-level performance assessment. While passive solutions improve thermal robustness, they may be insufficient under high-emission scenarios, highlighting the need for complementary adaptive or hybrid strategies.

Overall, the findings highlight the importance of considering the interaction between passive envelope characteristics, air infiltration conditions, future climate evolution, and spatial variability when assessing building thermal resilience. Although the quantitative outcomes remain dependent on the investigated case study and modelling assumptions, the identified trends and interaction mechanisms provide insight into the behaviour of residential buildings exposed to comparable hot arid and semi-arid climatic conditions. Future research should extend the proposed framework to additional building typologies, climatic contexts, and adaptation scenarios while incorporating dynamic ventilation, occupant behaviour, and hybrid passive–active solutions to further evaluate the robustness of climate-resilient building design strategies.

ABBREVIATIONS

IPCC Intergovernmental Panel on Climate Change
RCP Representative Concentration Pathway
EPS Expanded polystyrene
PCM Phase change materials
SHGC Solar heat gain coefficients
HD Heating discomfort
CD Cooling discomfort
EHD Extreme Heating discomfort
ECD Extreme Cooling discomfort
SHGC Solar Heat Gain Coefficient
ACH Air Change per Hour
CTF Conduction Transfer Function
Top Operative temperature

Author contributions: HK & OM: conceptualization, methodology, software, validation, formal analysis, writing—review and editing; **HK:** investigation, data curation, writing-original draft preparation, visualization; **OM:** resources, supervision, project administration. Both authors have read and agreed to the published version of the manuscript.

Funding: No funding source is reported for this study.

Ethical statement: The authors stated that this study did not require ethical approval, as it is based exclusively on numerical building energy simulations and publicly available climatic data. No human participants or animals were involved, and no personal or sensitive data were collected. Therefore, informed consent was not applicable.

AI statement: The authors stated that generative AI-based tools were used solely to improve the language and presentation of the manuscript. The authors critically reviewed and verified all content and take full responsibility for the scientific accuracy, analysis, interpretation, and conclusions presented in this work

Declaration of interest: No conflict of interest is declared by the authors.

Data sharing statement: Data supporting the findings and conclusions are available upon request from corresponding author.

REFERENCES

Abanda, F. H., & Byers, L. (2016). An investigation of the impact of building orientation on energy consumption in a domestic building using emerging BIM. *Energy, 97*, 517-527. https://doi.org/10.1016/j.energy.2015.12.135

Agence Marocaine pour l'Efficacité Energétique (AMEE). (2015). Règlement Thermique de Construction au Maroc (RTCM). Implementing Decree No. 2-13-874 of 15 October 2014 approving the General Construction Regulation establishing the energy performance requirements for buildings. Rabat, Morocco.

Amraoui, K., Ouanes, S., Daich, S., Reghiss, I., & Di Turi, S. (2025). Evaluating the effects of climate change on the thermal performance of residential buildings in hot and arid regions. *Buildings, 15*(23), Article 4378. https://doi.org/10.3390/buildings15234378

Arriazu-Ramos, A., Bes-Rastrollo, M., Sánchez-Ostiz Gutiérrez, A., & Monge-Barrio, A. (2022). Building parameters that influence overheating of apartment buildings in a temperate climate in Southern Europe. *Building and Environment, 228*, Article 109899. https://doi.org/10.1016/j.buildenv.2022.109899

Aruta, G., Ascione, F., Iovane, T., & Mastellone, M. (2025). Thermal resilience to climate change of energy retrofit technologies for building envelope. *Energy, 327*, Article 136489. https://doi.org/10.1016/j.energy.2025.136489

Ascione, F., Bianco, N., De Masi, R. F., de' Rossi, F., & Vanoli, G. P. (2014). Energy refurbishment of existing buildings through the use of phase change materials: Energy savings and indoor comfort in the cooling season. *Applied Energy, 113*, 990-1007. https://doi.org/10.1016/j.apenergy.2013.08.045

Barkhordarian, A., Bhend, J. H., & von Storch, H. (2011). Consistency of observed near surface temperature trends with climate change projections over the Mediterranean. *Climate Dynamics, 38*, 1695-1702. https://doi.org/10.1007/s00382-011-1060-y

Bastos Porsani, G., & Fernández Bandera, C. (2023). A case study of empirical validation of EnergyPlus infiltration models based on different wind data. *Buildings, 13*(2), 511. https://doi.org/10.3390/buildings13020511

Belcher, S. E., Hacker, J. N., & Powell, D. S. (2005). Constructing design weather data for future climates. *Building Services Engineering Research and Technology, 26*, 49-61. https://doi.org/10.1191/0143624405bt112oa

Choi, K., Park, S., Joe, J., Kim, S. I., Jo, J. H., Kim, E. J., & Cho, Y. H. (2023). Review of infiltration and airflow models in building energy simulations for providing guidelines to building energy modelers. *Renewable and Sustainable Energy Reviews, 181*, Article 113327. https://doi.org/10.1016/j.rser.2023.113327

Delgado-Gutierrez, E., Rubio-Bellido, C., & Canivell, J. (2025). Thermal comfort in social housing in Ecuador: Do free-running buildings work in current and future climates? *Buildings, 15*, Article 2018. https://doi.org/10.3390/buildings15122018

Diab, Z., Younes, J., & Ghaddar, N. (2025). Optimal passive interventions for enhancing resilience of naturally ventilated residential buildings in future climatic extremes. *Buildings, 15*, Article 4016. https://doi.org/10.3390/buildings15224016

Driouech, F., Elrhaz, K., Moufouma-Okia, W., Arjdal, K., & Balhane, S. (2020). Assessing future changes of climate extreme events in the CORDEX-MENA region using regional climate model ALADIN-Climate. *Earth Systems and Environment, 4*, 477-492. https://doi.org/10.1007/s41748-020-00169-3

Eddib, F., & Lamrani, M. A. (2019). Effect of thermal insulators on the thermal and energetic performance of the envelope of a house located in Marrakesh. *Alexandria Engineering Journal, 58*, 937-944. https://doi.org/10.1016/j.aej.2019.08.008

Flores-Larsen, S., Filippín, C., & Barea, G. (2019). Impact of climate change on energy use and bioclimatic design of residential buildings in the 21st century in Argentina. *Energy and Buildings, 184*, 216-229. https://doi.org/10.1016/j.enbuild.2018.12.015

Flores-Larsen, S., & Bre, F. (2026). Night-time urban heat exposure: Overheating and thermal resilience of South American bedrooms. *Building and Environment, 287*, Article 113757. https://doi.org/10.1016/j.buildenv.2025.113757

Fosas, D., Coley, D. A., Natarajan, S., Herrera, M., Fosas de Pando, M., & Ramallo-Gonzalez, A. (2018). Mitigation versus adaptation: Does insulating dwellings increase overheating risk? *Building and Environment, 143*, 740-759. https://doi.org/10.1016/j.buildenv.2018.07.033

Hatwaambo, S., Jain, P. C., Perers, B., & Karlsson, B. (2009). Projected beam irradiation at low latitudes using Meteonorm database. *Renewable Energy, 34*, 1394-1398. https://doi.org/10.1016/j.renene.2008.09.011

Intergovernmental Panel on Climate Change (IPCC). (2014). *Climate change 2014: Synthesis report*. IPCC.

Intergovernmental Panel on Climate Change (IPCC). (2021). *Climate change 2021: The physical science basis*. Cambridge University Press. https://doi.org/10.1017/9781009157896

Kasmi, H., & Mouhat, O. (2026). Parametric optimization of passive envelope design under 2020 and 2050 climate conditions: A case study of Marrakech. *Edelweiss Applied Science and Technology, 10*(4), 756-778. https://doi.org/10.55214/2576-8484.v10i4.12790

Kharbouch, Y. (2022). Effectiveness of phase change material in improving the summer thermal performance of an office building under future climate conditions: An investigation study for the Moroccan Mediterranean climate zone. *Journal of Energy Storage, 54*, Article 105253. https://doi.org/10.1016/j.est.2022.105253

Khechiba, A., Djaghrouri, D., Benabbas, M., Leccese, F., Rocca, M., & Salvadori, G. (2023). Balancing thermal comfort and energy consumption in residential buildings of desert areas: Impact of passive strategies. *Sustainability, 15*(10), Article 8383. https://doi.org/10.3390/su15108383

Kitsopoulou, A., Bellos, E., & Tzivanidis, C. (2024). An up-to-date review of passive building envelope technologies for sustainable design. *Energies, 17*(16), Article 4039. https://doi.org/10.3390/en17164039

Kutty, N. A., Barakat, D., Darsaleh, A. O., & Kim, Y. K. (2024). A systematic review of climate change implications on building energy consumption: Impacts and adaptation measures in hot urban desert climates. *Buildings, 14*(1), Article 13. https://doi.org/10.3390/buildings14010013

Kuznik, F., David, D., Johannes, K., & Roux, J. J. (2011). A review on phase change materials integrated in building walls. *Renewable and Sustainable Energy Reviews, 15*, 379-391. https://doi.org/10.1016/j.rser.2010.08.019

Machard, A., Inard, C., Alessandrini, J. M., Devys-Peyre, F., Martinez, S., Ribéron, J., & Pelé, C. (2023). Climate change influence on buildings dynamic thermal behavior during summer overheating periods: An in-depth sensitivity analysis. *Energy and Buildings, 284*, Article 112758. https://doi.org/10.1016/j.enbuild.2022.112758

Mohammed, M. A., Ismail M. Budaiwi, Al-Osta, M. A., Abdou, A. A. (2024). Thermo-environmental performance of modular building envelope panel technologies: A focused review. *Buildings, 14*(4), Article 917. https://doi.org/10.3390/buildings14040917

Ng, L. C., Persily, A. K., & Emmerich, S. J. (2015). Improving infiltration modeling in commercial building energy models. *Energy and Buildings, 88*, 316-323. https://doi.org/10.1016/j.enbuild.2014.11.078

Pérez-Carramiñana, C., Maciá-Mateu, A., Sirvent-García, G., & Lledó-Llorca, I. (2022). Study of natural ventilation and solar control strategies to improve energy efficiency and environmental quality in glazed heated swimming pools in a dry Mediterranean climate. *Sustainability, 14*(14), Article 8243. https://doi.org/10.3390/su14148243

Rodrigues, C., Rodrigues, E., Fernandes, M. S., & Tadeu, S. (2024). Prospective life cycle approach to buildings' adaptation for future climate and decarbonization scenarios. *Applied Energy, 372*, Article 123867. https://doi.org/10.1016/j.apenergy.2024.123867

Rodrigues, E., & Fernandes, M. S. (2020). Overheating risk in Mediterranean residential buildings: Comparison of current and future climate scenarios. *Applied Energy, 259*, Article 114110. https://doi.org/10.1016/j.apenergy.2019.114110

Romero-Recuero, I., Nestares-Nieto, B., & Serrano-Jiménez, A. (2025). Exploring the influence of shared socioeconomic pathway scenarios on school energy retrofits: An emphasis on the building envelope. *Applied Sciences, 15*(4), Article 1839. https://doi.org/10.3390/app15041839

Salata, F., Falasca, S., Ciancio, V., Curci, G., & de Wilde, P. (2023). Climate change related evolution of future building cooling energy demand in a Mediterranean country. *Energy and Buildings, 290*, Article 113112. https://doi.org/10.1016/j.enbuild.2023.113112

Salihi, M., Chhiti, Y., El Fiti, M., Harmen, Y., Chebak, A., & Jama, C. (2024). Enhancement of buildings energy efficiency using passive PCM coupled with natural ventilation in Moroccan climate zones. *Energy and Buildings, 315*, Article 114322. https://doi.org/10.1016/j.enbuild.2024.114322

Salihi, M., El Fiti, M., Harmen, Y., Chhiti, Y., Chebak, A., & M'Hamdi Alaoui, F. E. (2022). Evaluation of global energy performance of building walls integrating PCM: Numerical study in semi-arid climate in Morocco. *Case Studies in Construction Materials, 16*, Article e00979. https://doi.org/10.1016/j.cscm.2022.e00979

Spinoni, J., Barbosa, P., Bucchignani, E., Cassano, J., Cavazos, T., Christensen, J. H., Christensen, O. B., Coppola, E., Evans, J., Geyer, B., Giorgi, F., Hadjinicolaou, P., Jacob, D., Katzfey, J., Koenigk, T., Laprise, R., Lennard, C. J., Kurnaz, M. L., Li, D. ... Dosio, A. (2020). Future global meteorological drought hot spots: A study based on CORDEX data. *Journal of Climate, 33*, 3635-3661. https://doi.org/10.1175/JCLI-D-19-0084.1

Suresh, C., Hotta, T. K., & Saha, S. K. (2022). Phase change material incorporation techniques in building envelopes for enhancing thermal comfort: A review. *Energy and Buildings, 268*, Article 112225. https://doi.org/10.1016/j.enbuild.2022.112225

Tellache, A., Lazri, Y., Laafer, A., & Attia, S. (2025). Adaptive thermal comfort assessment in residential buildings under current and future Mediterranean climate scenarios. *Buildings, 15*, Article 3171. https://doi.org/10.3390/buildings15173171

Villano, F., Ascione, F., Cholewa, T., De Masi, R. F., Mauro, G. M., & Ruggiero, S. (2026). Climate change impact on envelope retrofit effectiveness: Energy and carbon performance of Italian residential and office buildings today vs. 2050. *Energy and Buildings, 357*, Article 117145. https://doi.org/10.1016/j.enbuild.2026.117145

Xie, X., Li, X., & Tian, Y. (2025). The impact of spatial models on the thermal environment of rural residential buildings during summer: A case study of Guanzhong Area, China. *Sustainability, 17*(18), Article 8431. https://doi.org/10.3390/su17188431

Younes, C., Shdid, C. A., & Bitsuamlak, G. (2011). Air infiltration through building envelopes: A review. *Journal of Building Physics, 35*, 267-302. https://doi.org/10.1177/1744259111423085

Zhang, C., Yu, Z., Zhu, Q., Shi, H., Yu, Z., & Xu, X. (2024). Air-permeable building envelopes for building ventilation and heat recovery: Research progress and future perspectives. *Buildings, 14*(1), Article 42. https://doi.org/10.3390/buildings14010042